

---

# Localization of Indium-111-Immunoglobulin G, Technetium-99m-Immunoglobulin G and Indium-111-Labeled White Blood Cells at Sites of Acute Bacterial Infection in Rabbits

Sandra A. Barrow, Wendy Graham, Shireen Jywook, Stephen C. Dragotakes, Howard F. Solomon, John W. Babich, Robert H. Rubin and Alan J. Fischman

*Division of Nuclear Medicine of the Department of Radiology and The Clinical Investigation Unit of the Medical Service, Massachusetts General Hospital; and the Departments of Radiology and Medicine, Harvard Medical School, Boston, Massachusetts; and the R. W. Johnson Pharmaceutical Research Institute, Spring House, Pennsylvania*

---

Biodistribution and infection imaging properties of  $^{111}\text{In}$ -DTPA-IgG,  $^{99\text{m}}\text{Tc}$ -hydrazino nicotinamide-IgG and  $^{111}\text{In}$ -WBC were compared in rabbits with *E. coli* infection. Groups of six rabbits were injected with 10 mCi of  $^{99\text{m}}\text{Tc}$ -IgG plus 0.5 mCi of  $^{111}\text{In}$ -IgG or 1 mCi of  $^{99\text{m}}\text{Tc}$ -IgG plus 0.05 mCi of  $^{111}\text{In}$ -WBC. At 4–5 and 18–20 hr, dual photon scintigrams were acquired. At both times, the distributions of  $^{99\text{m}}\text{Tc}$  and  $^{111}\text{In}$ -IgG were nearly identical. The sites of infection were well visualized with all three radiopharmaceuticals. In the early images, the target-to-background ratios (T/B) for  $^{111}\text{In}$  and  $^{99\text{m}}\text{Tc}$ -IgG determined by ROI analysis were  $1.95 \pm 0.26$  and  $2.57 \pm 0.38$  ( $p = \text{NS}$ ). In the delayed images, the T/B ratios increased ( $p < 0.01$ ) to  $3.56 \pm 0.49$  and  $4.90 \pm 0.98$ . At both times, the T/B ratios for  $^{111}\text{In}$ -WBC were higher ( $p < 0.01$ );  $4.17 \pm 0.78$  at 4–5 hr and  $8.52 \pm 1.52$  at 18–20 hr. These results indicate that all three agents yield excellent images of infection sites. Although  $^{111}\text{In}$ -WBC had higher T/B ratios, the ease of preparation of the radiolabeled proteins makes them attractive alternatives for infection imaging.

J Nucl Med 1993; 34:1975–1979

---

**T**he prompt, accurate and unequivocal identification of focal sites of infection is a critical step in the evaluation of patients with fever. Frequently, identification of the anatomic site of the process is more important than determining the microbial etiology of the lesion (1). Although conventional anatomic imaging studies such as plain radiographs, computed tomography and ultrasound are effective methods of infection localization, unequivocal lesion identification usually requires abscess formation. In contrast, most radionuclide techniques are more effective methods for delineating sites of infection at the phlegma stage. Currently, the most common radiopharmaceuticals for infec-

tion imaging are  $^{67}\text{Ga}$ -citrate (2,3),  $^{111}\text{In}$ -labeled leukocytes (4–6),  $^{99\text{m}}\text{Tc}$ -labeled leukocytes (7–9) and  $^{111}\text{In}$ -labeled human polyclonal immunoglobulin G (IgG) (10–11).

Although each of these agents can yield useful results in specific situations, considerable room for improvement exists. Gallium-67-citrate has proven to be useful for identifying sites of inflammation in the lungs and extremities, however, physiological excretion by the bowel limits the utility of this reagent for evaluating the abdomen. Indium-111 leukocytes have been a highly successful imaging agent, however, dosimetric considerations significantly limit the amount of radioactivity that can be administered, frequently resulting in poor quality images. Although much higher doses of  $^{99\text{m}}\text{Tc}$ -labeled leukocytes can be used, general applicability is limited by accumulation of radioactivity in nontarget organs;  $^{99\text{m}}\text{Tc}$ -HMPAO in bowel and  $^{99\text{m}}\text{Tc}$ -nanocolloid in reticuloendothelial system organs. In addition, all cell-based radiopharmaceuticals require complicated labeling methods which are associated with the potential danger of blood handling.

Most of the problems with  $^{67}\text{Ga}$  and radiolabeled cells are not associated with  $^{111}\text{In}$ -IgG. However, the high cost, lack of routine availability, unfavorable dosimetry and the relatively poor imaging characteristics of  $^{111}\text{In}$  limit the utility of this agent. Clearly, a  $^{99\text{m}}\text{Tc}$ -labeled form of IgG would eliminate most of these problems. Unfortunately, most of the current methods for radiolabeling proteins with  $^{99\text{m}}\text{Tc}$  either alter biodistribution or are relatively complicated procedures. Recently, we introduced a method for radiolabeling IgG with  $^{99\text{m}}\text{Tc}$  via a hydrazino nicotinamide derivatized intermediate (12). This preparation has been shown to have nearly identical biodistribution and imaging properties in infected rats and monkeys with focal sites of sterile inflammation. In the present study, we extend these investigations by comparing the infection localization properties of  $^{99\text{m}}\text{Tc}$ -IgG to  $^{111}\text{In}$ -labeled leukocytes in rabbits with focal sites of *E. coli* infection.

---

Received April 30, 1993; revision accepted July 5, 1993.  
For correspondence and reprints contact: Dr. Alan J. Fischman, Div. of Nuclear Medicine, Massachusetts General Hospital, Boston, MA 02114.

## MATERIALS AND METHODS

### Materials

Human polyclonal IgG (Gammimmune) was obtained from Cutter Laboratories (Emeryville, CA). Dimethylformamide (DMF) and p-nitro benzaldehyde were obtained from Aldrich Chemical Co. (St. Louis, MO). Bradford reagent was obtained from Sigma Chemical Co. (St. Louis, MO). All inorganic salts were obtained from Fisher Scientific Co. (Malvern, PA) and ITLC-sg chromatographic strips were obtained from Gelman Laboratories (Ann Arbor, MI).

### Radiopharmaceuticals

Indium-111-oxine and  $^{111}\text{In}$ -chloride were obtained from Amersham Inc. (Arlington Heights, IL) and  $^{99\text{m}}\text{Tc}$  generators were obtained from Dupont Radiopharmaceutical Division (N. Billerica, MA). Glucoheptonate kits were obtained from Squibb Diagnostics (Princeton, NJ) and were prepared according to the instructions of the manufacturer. IgG-DTPA (Macroscent<sup>®</sup>) was obtained from McNeil Inc. (Fort Washington, PA) and was radiolabeled according to the manufacturer's instructions.

### Technetium-99m-Labeled Immunoglobulin G

The nicotinyl hydrazine derivative of human polyclonal IgG (HYNIC-IgG) was prepared as described previously (12). Briefly, a fourfold molar excess of succinimidyl 6-hydrazino nicotinate hydrochloride (30 mM in DMF) was added dropwise to a stirred solution of IgG (1.0 g in 20 ml of 0.1 M phosphate buffer, pH 7.8) and the solution was stirred gently for 5 hr at room temperature. The mixture was dialysed against 10 mM citrate (pH 5.2) at 4°C and filtered through a 0.2- $\mu\text{m}$  filter. Protein concentration was determined by the Bradford method (13). The solution was diluted to 5 mg/ml with 100 mM NaCl/20 mM citrate/1% mannitol, (pH 5.2) and divided into 200- $\mu\text{l}$  aliquots and stored at -20°C. The number of hydrazino groups per IgG was determined by conversion to the corresponding hydrazone by reaction with p-nitrobenzaldehyde and measuring the optical density at 385 nm. Typically ~2.6 nicotinyl hydrazine groups were present per IgG.

HYNIC-IgG was radiolabeled with  $^{99\text{m}}\text{Tc}$  by addition of 20 mCi of  $^{99\text{m}}\text{Tc}$ -glucoheptonate to 0.5 ml of a solution of HYNIC-IgG, followed by incubation for 60 min at room temperature. Radiochemical purity was determined using ITLC-sg chromatographic strips, developed with 0.1 M of sodium citrate (pH 5.5). Typically >90% of the radioactivity was associated with antibody.

### Indium-111-Labeled Leukocytes

Fifty milliliters of heparinized whole blood, collected from a donor rabbit that was infected as described below was diluted 1:1 with Hesperan. Indium-111-labeled leukocytes were prepared by a previously described procedure (14,15) with the following modifications. Leukocyte rich plasma (LRP) was isolated by sedimenting the rabbit blood for 45 min. The LRP was centrifuged at 450 $\times$ g for 5 min. The white blood cell (WBC) pellet was resuspended in 10 ml of saline and allowed to stand for 60 min. The supernatant was then drawn off and the cells were resuspended in 5 ml of saline. Indium-111-oxine (500  $\mu\text{Ci}$ ) was added dropwise with agitation and the mixture was incubated for 60 min at 37°C with intermittent agitation. The cells were allowed to sediment and the pellet was suspended in platelet poor plasma.

### Infection Model

Male New Zealand white rabbits weighing 2.2–3.0 kg were used in all studies. *E. coli* from a single clinical isolate were grown overnight on trypticase soy agar plates and individual colonies

were diluted with sterile normal saline to produce a turbid suspension containing about  $1 \times 10^{11}$  organisms/0.5 ml (determined with a spectrophotometer). A 0.5-ml inoculum of the bacterial suspension was injected deep in the left thigh muscle of the rabbits.

Twenty-four hours after inoculation, rabbits with gross swelling in the infected thigh were injected with the radiopharmaceuticals through a lateral ear vein. Six animals were injected with a mixture of 1 mCi of  $^{99\text{m}}\text{Tc}$ -IgG (~0.25 mg protein) and 0.05 mCi of  $^{111}\text{In}$ -labeled WBC. Six additional animals were injected with a mixture of 10 mCi of  $^{99\text{m}}\text{Tc}$ -IgG (~2.5 mg protein) and 0.5 mCi of  $^{111}\text{In}$ -IgG (~0.60 mg protein).

## IMAGING AND BIODISTRIBUTION

### Animal Studies

At 4–5 and 18–20 hr following injection of the radiolabeled reagents, the animals were anesthetized with ketamine/xylazine (15.0 and 1.5 mg/kg) and anterior whole-body scintigrams were acquired using a large field of view gamma camera equipped with a parallel-hole, medium-energy collimator interfaced to a dedicated computer system (Technicare Gemini 700, Technicare 560, Solon, Ohio). Indium-111 and  $^{99\text{m}}\text{Tc}$  images were acquired simultaneously in dual photon-mode with 15% windows centered on photo-peaks at 140 keV for  $^{99\text{m}}\text{Tc}$  and 247 keV for  $^{111}\text{In}$ . At 4 hr after injection, two sets of images were acquired for a preset time of 5 min/view. At 20 hr after injection, the imaging time was extended to 10 min per view. Regions of interest were drawn over the area of infection and the contralateral normal muscle (background). The results were expressed as T/B ratios (inflamed thigh/contralateral thigh).

After acquiring the final images, the animals were killed with an overdose of sodium pentobarbital and biodistribution was determined. Samples of blood, heart, lung, liver, spleen, kidney, adrenal, stomach, GI tract, testes, bone, bone marrow, normal muscle and infected muscle (3–6 samples) were weighed and radioactivity was measured with a well-type gamma counter (LKB model 1282, Wallac Oy, Finland). To correct for radioactive decay and permit calculation of activity in each organ as a fraction of the administered dose, aliquots of the injected doses were counted simultaneously. The results were expressed as percent injected dose per gram (%ID/g).

### Phantom Studies

Phantom studies were performed to calculate the amount of crossover of 174 keV photons of  $^{111}\text{In}$  into the  $^{99\text{m}}\text{Tc}$  window and 140 keV photons of  $^{99\text{m}}\text{Tc}$  into the  $^{111}\text{In}$  window. Briefly, at the time that the animals were injected, samples of  $^{111}\text{In}$ -IgG and  $^{99\text{m}}\text{Tc}$ -DTPA were thoroughly mixed with 250 ml of saline in standard infusion bags in the same ratio injected in the rabbits. At 4 and 20 hr later, the phantoms were placed 5 cm apart on the imaging table and images in both windows were acquired. From ROIs drawn around each bag, crossover factors were calculated. These factors were used to correct the  $^{99\text{m}}\text{Tc}$  and  $^{111}\text{In}$  images.

## STATISTICAL METHODS

The results of the imaging and biodistribution studies were evaluated statistically by analysis of variance (ANOVA) followed by Duncan's new multiple range test (16). For the T/B data, a two-way ANOVA with a linear model in which time after injection and radiopharmaceutical ( $^{111}\text{In-IgG}$ ,  $^{99\text{m}}\text{Tc-IgG}$  or  $^{111}\text{In-WBC}$ ) were the classification variables employed (T/B = Time + Radiopharmaceutical + Time \* Radiopharmaceutical). For the biodistribution data, two-way ANOVA with a linear model in which organ and IgG preparation ( $^{99\text{m}}\text{Tc}$  or  $^{111}\text{In}$ ) were the classification variables was employed (%ID/g = Organ + Prep. + Organ \* Prep). In addition, the T/B for  $^{111}\text{In-IgG}$  versus  $^{99\text{m}}\text{Tc-IgG}$  and  $^{111}\text{In-WBC}$  versus  $^{99\text{m}}\text{Tc-IgG}$  were compared by linear regression. All results were expressed as mean  $\pm$  s.e.m.

## RESULTS

### Phantom Studies

The phantom studies indicated that at 4 hr after injection of the radiopharmaceuticals, ~5% of the photons detected in the  $^{99\text{m}}\text{Tc}$  window were contributed by  $^{111}\text{In}$ . At 20 hr after injection, ~17% of the photons detected in the  $^{99\text{m}}\text{Tc}$  window were contributed by  $^{111}\text{In}$ . At both imaging times <2% of the photons detected in the  $^{111}\text{In}$  window were contributed by  $^{99\text{m}}\text{Tc}$ . All imaging data was corrected for these spillover effects.

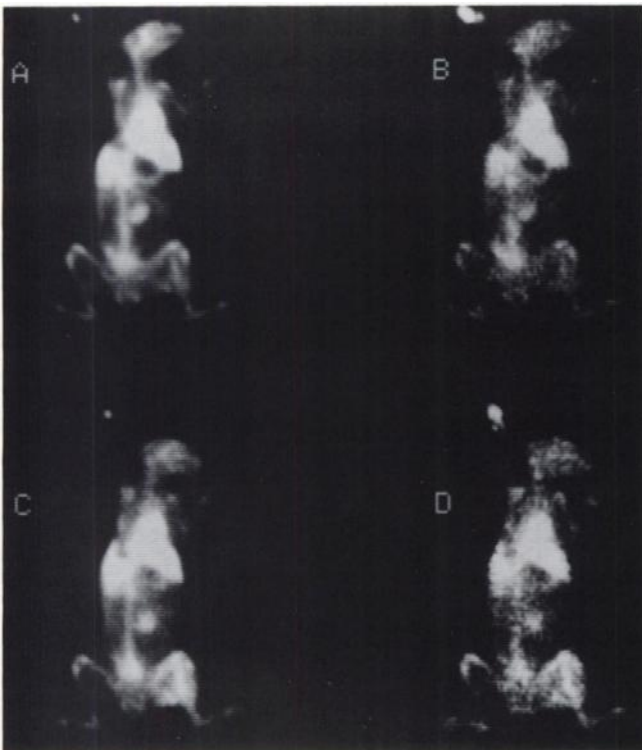


**FIGURE 1.** Gamma camera images of a rabbit with *E. coli* deep thigh infections at 4 and 20 hr after co-injection of  $^{99\text{m}}\text{Tc}$  and  $^{111}\text{In-IgG}$ . (A)  $^{99\text{m}}\text{Tc-IgG}$  at 4 hr. (B)  $^{111}\text{In-IgG}$  at 4 hr. (C)  $^{99\text{m}}\text{Tc-IgG}$  at 20 hr. (D)  $^{111}\text{In-IgG}$  at 20 hr. The  $^{99\text{m}}\text{Tc}$  images were corrected for  $^{111}\text{In}$  photons in the  $^{99\text{m}}\text{Tc}$  window and images B–D were normalized to the total number of counts in image A. Infections were established 24 hr prior to injection.

**TABLE 1**  
Biodistribution of Technetium-99m and Indium-111-IgG in the Rabbit\*

	$^{99\text{m}}\text{Tc-IgG}$	$^{111}\text{In-IgG}$
Blood	0.109 $\pm$ 0.019	0.084 $\pm$ 0.026
Heart	0.043 $\pm$ 0.007	0.036 $\pm$ 0.011
Lung	0.048 $\pm$ 0.009	0.037 $\pm$ 0.015
Liver	0.110 $\pm$ 0.018	0.094 $\pm$ 0.019
Spleen	0.097 $\pm$ 0.018	0.086 $\pm$ 0.034
Kidney	0.069 $\pm$ 0.009	0.060 $\pm$ 0.023
Adrenal	0.080 $\pm$ 0.014	0.119 $\pm$ 0.048
Stomach	0.012 $\pm$ 0.002	0.011 $\pm$ 0.004
GI tract	0.016 $\pm$ 0.003	0.014 $\pm$ 0.003
Testes	0.036 $\pm$ 0.006	0.028 $\pm$ 0.012
Muscle	0.002 $\pm$ 0.0003	0.002 $\pm$ 0.0006
Marrow	0.066 $\pm$ 0.016	0.104 $\pm$ 0.038
Bone	0.015 $\pm$ 0.002	0.012 $\pm$ 0.004

\*(%ID/g, mean  $\pm$  s.e.m.)

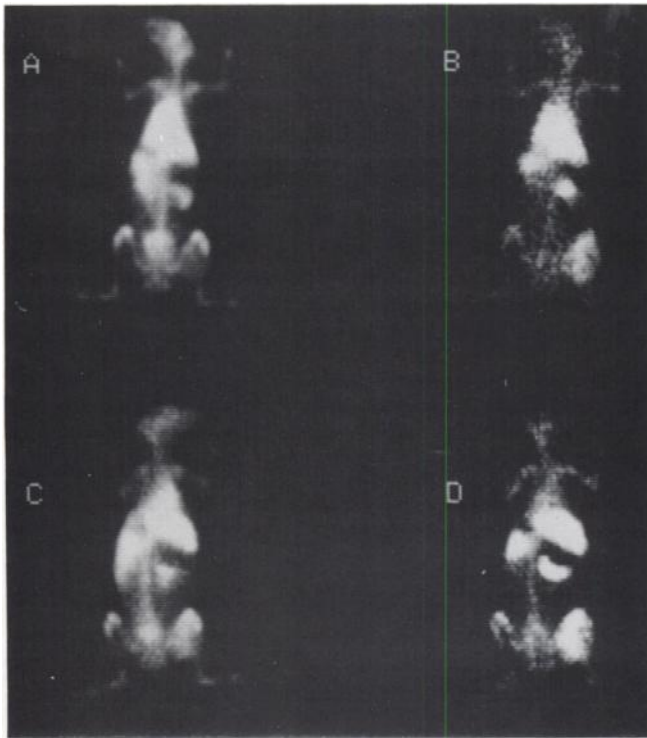
### Biodistribution of Technetium-99m-IgG and Indium-111-IgG

Figure 1 shows representative, crossover corrected, anterior images of a rabbit at 4 and 20 hr after co-injection of  $^{99\text{m}}\text{Tc-IgG}$  and  $^{111}\text{In-IgG}$ . At both imaging times, the overall biodistributions of the two radiopharmaceuticals were nearly identical. High concentrations of both agents were detected in the cardiac blood pool, vascular structures, liver, spleen and kidney. Concentration of both tracers were lower in lung, muscle, bone and gastrointestinal tract.

The biodistributions of  $^{99\text{m}}\text{Tc}$  and  $^{111}\text{In}$ -labeled IgG (%ID/g) determined by direct tissue radioactivity measurements at 20 hr after injection are shown in Table 1. Analysis of variance demonstrated significant main effects of organ ( $F_{12,104} = 6.36$ ;  $p < 0.0001$ ). However the main effects of labeling method ( $F_{1,104} = 0.91$ ;  $p > 0.35$ ), and the organ by labeling method interaction ( $F_{12,104} = 0.61$ ;  $p > 0.80$ ) were not significant. A significant difference in the concentration of  $^{111}\text{In-IgG}$  and  $^{99\text{m}}\text{Tc-IgG}$  was not detected in any tissue that was examined.

### Radiotracer Accumulation at Infection Sites

Figure 2 shows representative crossover corrected, anterior images of a rabbit at 4 and 20 hr after co-injection of  $^{99\text{m}}\text{Tc-IgG}$  and  $^{111}\text{In-WBC}$ . By comparing Figures 1 and 2 it is apparent that all three radiopharmaceuticals localize at sites of infection to a significant extent at both 4 and 20 hr after injection. With all three agents, greatest accumulation occurred at 20 hr. At both imaging times, the level of accumulation of radioactivity at the site of infection was greatest with the radiolabeled WBC and the degree of accumulation of IgG was independent of the radionuclide used for labeling. The T/B ratios for the three radiopharmaceuticals are summarized in Figure 3. Analysis of variance showed significant main effects of radiopharmaceutical ( $F_{2,30} = 7.97$ ,  $p < 0.005$ ) and time after injection ( $F_{1,30} = 13.24$ ,  $p < 0.005$ ). However, the radiopharmaceutical by time interaction was not significant ( $F_{2,30} = 1.16$ ,  $p > 0.30$ ).



**FIGURE 2.** Gamma camera images of a rabbit with an *E. coli* deep thigh infection at 4 and 20 hr after co-injection of  $^{99m}\text{Tc}$ -IgG and  $^{111}\text{In}$ -WBC (A)  $^{99m}\text{Tc}$ -IgG at 4 hr. (B)  $^{111}\text{In}$ -WBC at 4 hr. (C)  $^{99m}\text{Tc}$ -IgG at 20 hr. (D)  $^{111}\text{In}$ -WBC at 20 hr. The  $^{99m}\text{Tc}$  images were corrected for  $^{111}\text{In}$  photons in the  $^{99m}\text{Tc}$  window and images B-D were normalized to the total number of counts in image A. Infections were established 24 hr prior to injection.

The T/B ratio for all three agents increased significantly with time ( $p < 0.05$ ) and at both imaging times the T/B ratio for  $^{111}\text{In}$ -WBC was significantly greater ( $p < 0.01$ ) than for  $^{99m}\text{Tc}$  or  $^{111}\text{In}$ -labeled IgG. At both imaging times, the T/B ratios for  $^{99m}\text{Tc}$  and  $^{111}\text{In}$ -labeled IgG were not significantly different.

Figure 4 shows a plot of the infected to normal tissue ratios (T/B) of  $^{99m}\text{Tc}$ -IgG and  $^{111}\text{In}$ -IgG determined by direct radioactivity measurements on samples of excised tissues at 20 hr after injection. Regression analysis demonstrated that the T/B ratios for the two radiopharmaceuticals were highly correlated:  $T/B(^{99m}\text{Tc}) = 1.15 \pm 0.074 * (T/B)^{111}\text{In} + 3.45 \pm 1.22$  ( $r^2 = 0.93$ ,  $df = 28$ ). In contrast, a similar comparison for  $^{99m}\text{Tc}$ -IgG and  $^{111}\text{In}$ -WBC failed to demonstrate a significant correlation ( $r^2 = 0.081$ ).

## DISCUSSION

Indium-labeled human polyclonal IgG and WBC have been demonstrated to be useful radiopharmaceuticals for localizing focal sites of infection/inflammation. However, since both reagents are labeled with  $^{111}\text{In}$ , direct comparison of their properties by co-injection in the same subject has not been possible. The recent development of  $^{99m}\text{Tc}$ -IgG has eliminated this problem. Although  $^{111}\text{In}$  and  $^{99m}\text{Tc}$ -IgG have been demonstrated to have nearly identical biodistributions and infection imaging properties in rats (12),

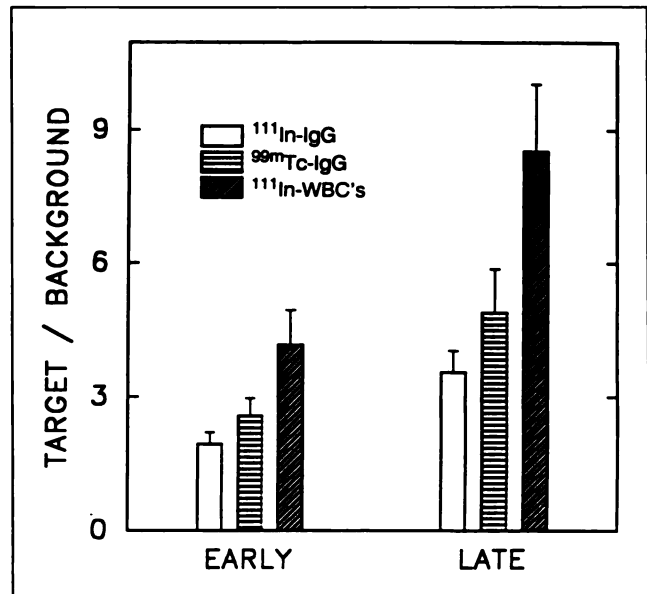


**FIGURE 3.** Target-to-background ratios of  $^{99m}\text{Tc}$ -IgG,  $^{111}\text{In}$ -IgG and  $^{111}\text{In}$ -WBC at 4-5 and 18-20 hr after injection. Each point is the mean  $\pm$  s.e.m. for six animals. In all cases, the animals were infected 24 hr prior to injection.

this might not be applicable to all species. In the present study, we verified that  $^{111}\text{In}$  and  $^{99m}\text{Tc}$ -IgG have similar efficacies for infection localization in rabbits with acute *E. coli* infections and compared  $^{99m}\text{Tc}$ -IgG with  $^{111}\text{In}$ -WBC.

Indium-111 and  $^{99m}\text{Tc}$ -IgG have very similar imaging and biodistribution properties. Even though the technetium-labeled antibody has slightly better targeting properties, this difference is unlikely to be of clinical significance. Although  $^{111}\text{In}$ -WBC had greater T/B ratios than radiola-

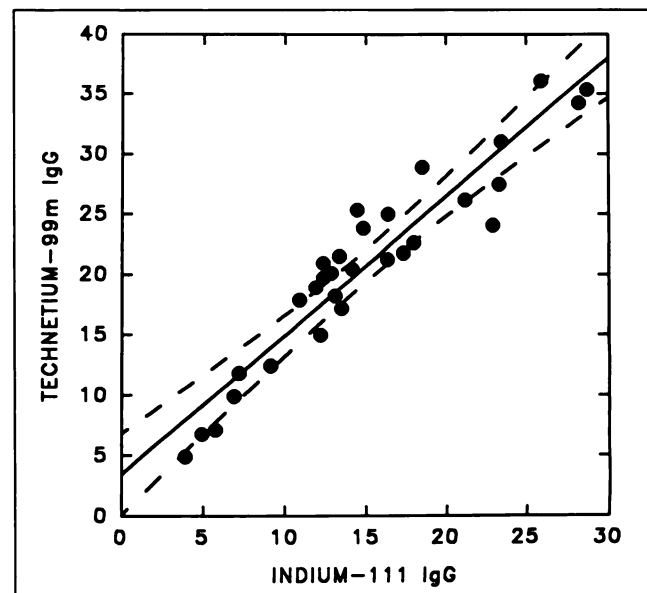


**FIGURE 4.** Infected-to-normal tissue ratios (T/B) of  $^{99m}\text{Tc}$ -IgG and  $^{111}\text{In}$ -IgG determined by direct radioactivity measurements on excised samples of normal and infected muscle (3-6 samples/animal) at 20 hr after injection. The dashed lines are the 99% confidence limits.

beled IgG at both imaging times, the difference was modest. This observation does not conflict with the results of previous studies which demonstrated rapid clearance of  $^{99m}\text{Tc}$ -IgG from infected and background tissues since a different radiolabeling method was used in our study (17,18). In a recent report, the localization of  $^{125}\text{I}$ -IgG was compared to  $^{111}\text{In}$ -WBC (19). In this study, the T/B ratio for the labeled cells was ~10-fold higher than radiolabeled IgG in dogs with *E. coli* infection. Unfortunately, it is difficult to directly compare the results of this study with ours, since of the 24 dogs that were injected with  $^{111}\text{In}$ -WBC, only 8 received radiolabeled IgG. Considering the reported variability of the T/B ratios with  $^{111}\text{In}$ -WBC, the fact that T/B ratios for  $^{111}\text{In}$ -WBC in the subset of animals injected with  $^{125}\text{I}$ -IgG was not reported makes comparison difficult.

An interesting observation of the present study is the lack of correlation between IgG and radiolabeled WBC accumulation at sites of infection. This adds support to the notion that the mechanism of IgG accumulation is primarily due to increased penetration and decreased clearance from the expanded protein space of inflammatory lesions (20,21). If binding to Fc receptors on inflammatory cells made a significant contribution to IgG localization at sites of inflammation, accumulations of the two radiopharmaceuticals would be expected to be significantly correlated (22,23).

Since clinical experience with  $^{111}\text{In}$ -IgG has indicated that most inflammatory lesions can be detected within 24 hr after injection (10,11),  $^{99m}\text{Tc}$ -IgG should be an equally effective imaging agent. From extensive biodistribution data in rats, MIRDose calculations indicate that ~20 mCi of  $^{99m}\text{Tc}$ -IgG can be injected without delivering a radiation burden in excess of 2 rads to any organ (unpublished results). Based on the physical properties of  $^{111}\text{In}$  and  $^{99m}\text{Tc}$ , nearly threefold greater photon flux should be present at the lesion site 19 hr postinjection if tenfold more  $^{99m}\text{Tc}$  IgG is initially injected. In addition, due to the superior intrinsic imaging properties of  $^{99m}\text{Tc}$  and the greater photon fluxes at early times, the technetium-labeled protein will provide much better quality images for the detection of expanded protein space at sites of inflammation, particularly if SPECT is used.

In conclusion, the results of this study strongly indicate that  $^{99m}\text{Tc}$ -IgG labeled via the hydrazino nicotinamide intermediate is equivalent to  $^{111}\text{In}$ -IgG for imaging focal sites of inflammation in rabbits. Although  $^{111}\text{In}$ -WBC yielded higher T/B ratios at both imaging times, the ease of preparation and lack of blood handling with the radiolabeled proteins makes them useful alternatives for infection imaging.

## ACKNOWLEDGMENT

This study was supported in part by a grant from the R. W. Johnson Pharmaceutical Research Spring House, PA.

## REFERENCES

- Ahrenholz OH, Simmons RL. Pancreatitis and other intra-abdominal infections. In: Howard RJ, Simmons RL, eds. *Surgical infectious diseases, second edition*. Norwalk, Conn: Appleton and Lange; 1988;605-646.
- Hoffer P. Gallium and infection. *J Nucl Med* 1980;21:484-488.
- Ebright JR, Soin JS, Manoli RS. The gallium scan: problems and misuse in examination of patients with suspected infection. *Arch Intern Med* 1982; 142:246-254.
- McAfee JG, Samin A. In-111-labeled leukocytes: a review of problems in image interpretation. *Radiology* 1985;155:221-229.
- Froelich JW, Swanson D. Imaging of inflammatory processes with labeled cells. *Semin Nucl Med* 1984;14:128-140.
- Thakur ML. Gallium-67 and indium-111 radiopharmaceuticals. *Int J Appl Radiat Isot* 1977;28:183-201.
- Ruther W, Hotze A, Moller F, Bockisch A, Heitzmann P, Biersack HJ. Diagnosis of bone and joint infection by leucocyte scintigraphy. A comparative study with  $^{99m}\text{Tc}$ -HMPAO-labeled leukocytes,  $^{99m}\text{Tc}$ -labeled anti-granulocyte antibodies and  $^{99m}\text{Tc}$ -labeled nanocolloid. *Arch Orthop Trauma Surg* 1990;110:26-32.
- Vorne M, Lantto T, Paakinen S, Salo S, Soini I. Clinical comparison of  $^{99m}\text{Tc}$ -HMPAO-labeled leukocytes and  $^{99m}\text{Tc}$ -nanocolloid in the detection of inflammation. *Acta Radiol* 1989;30:633-637.
- Peters AM, Roddie ME, Danpure HJ, et al.  $^{99m}\text{Tc}$ -HMPAO-labeled leukocytes: comparison with  $^{111}\text{In}$ -tropolonate labeled granulocytes. *Nucl Med Commun* 1988;9:449-463.
- Fischman AJ, Rubin RH, Khaw BA, et al. Detection of acute inflammation with  $^{111}\text{In}$ -labeled nonspecific polyclonal IgG. *Semin Nucl Med* 1988;18: 335-344.
- Rubin RH, Fischman AJ, Callahan RJ, et al. The utility of  $^{111}\text{In}$ -labeled nonspecific immunoglobulin scanning in the detection of focal inflammation. *N Engl J Med* 1989;321:935-940.
- Abrams MJ, Juweid M, tenKate CI, et al. Technetium-99m human polyclonal IgG radiolabeled via the hydrazino nicotinamide derivative for imaging focal sites of infection in rats. *J Nucl Med* 1990;31:2022-2028.
- Bradford MM. A rapid and sensitive method for the quantitation of microgram quantities of protein utilizing the principle of protein-dye binding. *Anal Biochem* 1976;72:248-254.
- McAfee JG, Gagne GM, Subramanian G, et al. Distribution of leukocytes labeled with  $^{111}\text{In}$ -oxime in dogs with acute inflammatory lesion. *J Nucl Med* 1980;21:1059-1068.
- McAfee JG, Subramanian G, Gagne G. Technique of leukocyte harvesting and labeling: problems and perspectives. *Semin Nucl Med* 1984;14:83-106.
- Duncan DB. Multiple range tests and multiple F-tests. *Biometrics* 1955;11: 1-42.
- Buscomb JR, Lui D, Ensing G, Jong R de, Ell PJ. Technetium-99m-human immunoglobulin (HIG)-first results of a new agent for the localization of infection and inflammation. *Eur J Nucl Med* 1990;16:649-655.
- Corstens FHM, Claessens AMJ. Imaging inflammation with human polyclonal immunoglobulin: not looked for but discovered. *Eur J Nucl Med* 1992;19:155-158.
- McAfee JG, Gagne G, Subramanian G, Schneider RF. The localization of indium-111-leukocytes, gallium-67, polyclonal IgG and other radioactive agents in acute focal inflammatory lesions. *J Nucl Med* 1991;32:2126-2131.
- Morrell EM, Tompkins RG, Fischman AJ, et al. An autoradiographic method for quantitation of radiolabeled proteins in tissue using indium-111. *J Nucl Med* 1989;30:1538-1545.
- Juweid M, Strauss HW, Yaoito H, Rubin RH, Fischman AJ. Accumulation of immunoglobulin G at focal sites of infection. *Eur J Nucl Med* 1992;19: 159-165.
- Fischman AJ, Rubin RH, White JA, et al. Localization of Fc and Fab fragments of nonspecific polyclonal IgG at focal sites of infection. *J Nucl Med* 1990;31:1199-1205.
- Fischman AJ, Fucello AJ, Pellegrino-Gensey JL, et al. Effect of carbohydrate modification on the localization of human polyclonal IgG at focal sites of bacterial infection. *J Nucl Med* 1992;33:1378-1382.